HHS Public Access

Author manuscript

J Magn Reson Imaging. Author manuscript; available in PMC 2017 November 01.

Published in final edited form as:

J Magn Reson Imaging. 2016 November ; 44(5): 1244–1255. doi:10.1002/jmri.25248.

Measurement of Arteriolar Blood Volume in Brain Tumors Using MRI without Exogenous Contrast Agent Administration at 7T

Yuankui Wu, M.D.[1,2,3], **Shruti Agarwal, Ph.D.**[4], **Craig K. Jones, Ph.D.**[2,3], **Andrew G. Webb, Ph.D.**[5], **Peter C. M. van Zijl, Ph.D.**[2,3], **Jun Hua, Ph.D.**[*,2,3], and **Jay J. Pillai, M.D.**[*,4]

[1]Department of Medical Imaging, Nanfang Hospital, Southern Medical University, Guangzhou, P.R. China [2]Division of MR Research, Russell H. Morgan Department of Radiology and Radiological Science, Johns Hopkins University School of Medicine, Baltimore, MD, USA [3]F. M. Kirby Research Center for Functional Brain Imaging, Kennedy Krieger Institute, Baltimore, MD, USA [4]Division of Neuroradiology, Russell H. Morgan Department of Radiology and Radiological Science, Johns Hopkins University School of Medicine, Baltimore, MD, USA [5]Department of Radiology, C.J.Gorter Center for High Field MRI, Leiden, University Medical Center, Leiden, The Netherlands.

Abstract

Purpose—Arteriolar cerebral-blood-volume (CBVa) is an important perfusion parameter that can be measured using inflow-based vascular-space-occupancy (iVASO) MRI without exogenous contrast agent administration. The purpose of this study is to assess the potential diagnostic value of CBVa in brain tumor patients by comparing it with total-CBV (including arterial, capillary and venous vessels) measured by dynamic-susceptibility-contrast (DSC) MRI.

Methods—Twelve brain tumor patients were scanned using iVASO (on 7T as part of a research project) and DSC (on 3T as part of routine clinical protocols) MRI. Region-of-interest analysis was performed to compare the resulting perfusion measures between tumoral and contralateral regions, and to evaluate their associations with tumor grades.

Results—CBVa measured by iVASO-MRI significantly correlated with WHO grade (ρ=0.37, P=0.04). Total-CBV measured by DSC-MRI showed a trend of correlation with WHO grade (ρ=0.28, P=0.5). Signal-to-noise ratio was comparable (P>0.1) between the two methods, while contrast-to-noise ratio between tumoral and contralateral regions was higher in iVASO-CBVa than DSC-CBV in WHO II/III patients (P<0.05) but comparable in WHO IV patients (P>0.1). A trend of positive correlation between DSC-CBV and iVASO-CBVa was observed (R^2=0.28, P=0.07).

Conclusion—In this initial patient study, CBVa demonstrated a stronger correlation with WHO grade than total-CBV. Further investigation with a larger cohort is warranted to validate whether CBVa can be a better classifier than total-CBV for the stratification of brain tumors, and whether

[*]**Corresponding Authors:** Jun Hua, Ph.D., F.M. Kirby Research Center for Functional Brain Imaging, Kennedy Krieger Institute, Department of Radiology, Johns Hopkins University School of Medicine, 707 N Broadway, Baltimore, MD, 21205, jhua@mri.jhu.edu, Tel: 443-923-3848, Fax: 443-923-9505, Jay J. Pillai, M.D., Division of Neuroradiology, Russell H. Morgan Department of Radiology and Radiological Science, The Johns Hopkins University School of Medicine, The Johns Hopkins Hospital, Phipps B-100, 1800 Orleans Street, Baltimore, MD 21287. jpillai1@jhmi.edu, Phone: (410) 614-3020, Fax: (410)614-1213.

iVASO-MRI can be a useful alternative method for the assessment of tumor perfusion, especially when exogenous contrast agent administration is difficult in certain patient populations.

Keywords

Tumor perfusion; microvasculature; cerebral blood volume; vascular-space-occupancy; high field; brain tumor

Introduction

The degree of neovascularization and the ability to recruit vessels and develop a vascular network for growth and infiltration are important factors in the evaluation of the malignancy of brain tumors and establishment of their prognosis (1-4). Vasculature also profoundly affects drug delivery as well as radiotherapy effectiveness (5). Cerebral blood volume (CBV) and flow (CBF) are sensitive indicators of the homeostasis of the microvasculature in the brain. As a critical step of tumor growth and survival, new blood vessels are formed to deliver oxygen, glucose, various growth factors and to provide routes for tumor cell migration (4); this results in changes in the overall number of blood vessels, and thus total CBV values in neoplastic brain tissue. It has been demonstrated that CBV alterations may be more sensitive and may occur earlier than CBF changes in tumors (6). Significant correlations between total CBV and glucose uptake have been reported in human gliomas (7). These findings suggest that tumor CBV may be a useful quantitative measure for the diagnosis, treatment planning, and longitudinal monitoring of patients with central nervous system tumors.

Dynamic susceptibility contrast (DSC) MRI is currently the standard imaging technique for the measurement of cerebral perfusion in brain tumor patients (8). In DSC MRI, fast image acquisition is performed to measure dynamic signal changes following intravenous injection of an exogenous contrast agent, from which several parameters including CBV, CBF, and mean transit time (MTT) can be derived (9). A number of studies have demonstrated the diagnostic value of such perfusion parameters for predicting tumor grade and probing tumor physiology and response to therapeutics (10-12). On the other hand, one main difficulty in DSC MRI is the estimation of the arterial input function (AIF). In addition, the requirement of exogenous contrast agent administration in DSC MRI furnishes a relatively short time window for data acquisition, and makes it logistically inconvenient in certain cases. One common type of contrast media, gadolinium based contrast agents, have been associated with nephrogenic systemic fibrosis in subjects with renal insufficiency (13,14). More recently, frequent gadolinium exposure was shown to result in permanent brain deposits of such contrast agents even in subjects with normal renal function (15). Renal dysfunction often occurs in tumor patients undergoing chemotherapy, which makes follow-up evaluation of tissue perfusion during chemotherapy difficult with DSC MRI (16,17).

Recently, the inflow-based vascular-space-occupancy (iVASO) MRI technique has been developed, which is able to quantify absolute arteriolar CBV (CBVa) in the brain without the need for exogenous contrast agent (18-24). In iVASO MRI, proton spins in the water molecules in blood are exploited as intrinsic endogenous contrast agents, which can be

manipulated by applying spatially selective radiofrequency (RF) inversion pulses. CBVa can be quantified from the difference signal between a scan with arterial blood signal selectively zeroed out (nulled) and a control scan without blood nulling (18,20). As vascular transit times may vary in different brain regions, iVASO images are acquired at multiple post-inversion delay times to account for this heterogeneity. A quantitative theory has been derived to calculate absolute CBVa and arterial transit time (ATT) from iVASO data (18). Crushing gradients can be incorporated in iVASO MRI to suppress signals from large arteries and to sensitize this method to CBVa predominantly in the pial arteries and arterioles. Although the pulse sequence of iVASO MRI is similar to some of the arterial spin labeling (ASL) methods (25-28) for CBF measurement, the underlying contrast mechanisms of iVASO and ASL differ fundamentally. ASL measures tissue perfusion (i.e. CBF) based on the exchange between labeled blood water and tissue water protons in the capillary bed. Therefore, a proper ASL acquisition needs to eliminate unwanted arterial blood effects (29-31). On the other hand, iVASO is designed to highlight the vascular contribution from the arterial and arteriolar (with crushing gradients) compartment, in which negligible water exchange between blood and tissue occurs due to limited permeability of the vessel wall. The predominant arterial origin of iVASO signal was validated in our previous study by measuring the transverse relaxation times (T2*/T2) of iVASO difference signals (Figure 5 in (18)), which are highly oxygenation level dependent (32). Besides, the arterial origin is also supported by the observation that the iVASO signal changes during functional stimulation uniformly preceded the changes in total CBV (the sum of arterial, capillary and venous CBV) (19), which is congruent with results from animal studies using optical imaging showing earlier hemodynamic responses in arterioles upon neuronal activation (33,34).

Physiologically, arterioles and pial arteries are the most actively regulated blood vessels in the microvasculature (35-37). There is evidence that generation of arterioles occurs before capillary growth and CBF changes in angiogenesis (38). Therefore, the ability to measure arteriolar CBV separately from the rest of the microvasculature (capillaries and venous vessels) may furnish information that is not obtainable from total CBV and CBF measures, and may make the measurement more sensitive because it is more specific. In the present study, we will evaluate the potential clinical value of CBVa for the assessment of tumor perfusion by applying iVASO MRI to measure CBVa and ATT in primary cerebral glioma patients and comparing the results with total CBV and MTT measured by DSC MRI in the same patients. We will assess the advantages and limitations of each approach in the context of brain tumor imaging.

Materials and Methods

Patients

This study was approved by the Johns Hopkins Institutional Review Board, and written informed consent was obtained from each patient for the research component. Fourteen brain tumor patients were recruited for this study among which twelve patients completed all scans with satisfactory image quality (nine male, three female; age 21-69 years, 38.4±18.2 years; see Table 1 for more information).

According to the World Health Organization (WHO) 4-tier classification of gliomas, three grade IV glioblastomas, two grade III anaplastic astrocytomas, one grade III anaplastic oligodendroglioma, four grade II oligodendrogliomas, and two grade II oligoastrocytomas were studied. All diagnoses were confirmed by histopathology performed by a neuropathologist with more than 10 years of related experience. The areas targeted for biopsy or resection in all cases were the areas that were considered to be the most highly cellular regions (based on imaging data, described in the MRI sub-section next). None of the patients had undergone surgical resection or chemoradiation therapy prior to these scans, and none had other neurologic history, or history of vascular diseases.

MRI

Each subject underwent two MRI sessions: a clinical session with DSC MRI and a research session with iVASO MRI, which were performed on the same day (8 patients) or on two different days within a week (4 patients). The clinical MRI session was conducted on a 3.0 Tesla (3T) Siemens Tim Trio human MRI scanner (Siemens Medical Solutions, Erlangen, German) equipped with a 12-channel head matrix coil in the Johns Hopkins Hospital. The following scans were performed as part of the standard clinical brain tumor functional imaging MRI protocol: three-dimensional (3D) T1-weighted magnetization-prepared rapid acquisition gradient-echo (MPRAGE) scan (TR/TI/TE = 2300/900/3.5 ms, voxel = 1mm isotropic, 176 slices); two-dimensional (2D) T2-weighted fluid attenuated inversion recovery (FLAIR) scan (TR/TI/TE = 9000/2500/116 ms, voxel = 0.7×0.7×3 mm^3, 50 slices). DSC perfusion images were acquired following the administration of Gd-DTPA contrast agent with gradient-echo (GRE) echo-planar-imaging (EPI) readout, TR/TE=1640/35 ms, voxel = 2×2×4 mm^3, 20 slices, 45 dynamics, 1.5 minutes.

The research MRI session was performed on a 7.0 Tesla (7T) Philips human MRI scanner (Philips Healthcare, Best, The Netherlands). A head-only quadrature coil and a 32-channel phased-array head coil (Nova Medical, Wilmington, MA) were used for RF transmit and reception, respectively. A pair of pads filled with high dielectric constant materials (39) were placed on the lateral sides of the subjects' head inside the coil to mitigate B1 field inhomogeneity (40). T1-weighted anatomical images were acquired with a 3D MPRAGE sequence (TR/TI/TE = 4500/563/2 ms, voxel = 1 mm isotropic, 180 slices). CBVa maps were acquired using iVASO MRI in single-slice mode with a GRE EPI readout. The basic principle of iVASO MRI has been described in the Introduction, and more details can be found in our previous work (18). The iVASO slice was prescribed in each patient on the anatomical images and was centered in a portion of the tumor that included the most cellular regions based on anatomical and DSC perfusion (from 3T clinical session) images, and in cases of enhancing tumor included the enhancing components. We were careful to avoid regions of necrosis in the sampled slices. Interleaved nulling and control iVASO images were acquired at six different post-inversion delay times (TI), from which voxel-wise CBVa and ATT values were calculated using the iVASO theory (18). The inversion pulses used in iVASO were optimized in our previous 7T work on the same scanner (41). The following iVASO parameters were used: TR/TI = 10000/1626, 5000/1382, 3100/1081, 2000/797, 1700/691, and 1300/563 ms (TI calculated based on a blood T1 value of 2587 ms), number of interleaves = 3, 5, 8, 10, 15, 15, respectively; TE = 16 ms; field of view (FOV) = 192×192

mm^2, voxel = 2.5×2.5×3 mm^3; parallel imaging acceleration (SENSE) = 3; crusher gradients of b = 0.3 s/mm^2 and Venc = 10 cm/s in the z-direction (as average blood flow velocity in pial arteries is in the range of 1-5 cm/s (42,43), Venc = 10 cm/s was chosen as an approximate upper limit for the target vessels in this study). The iVASO scaling factor M0 for absolute CBVa quantification was determined in a separate reference scan without inversion (TR = 20 s, other parameters identical) following the iVASO scans (18). The total duration of all iVASO related scans added up to 7 minutes for each patient.

Image analysis

All data were pre-processed using the statistical parametric mapping (SPM, Wellcome Trust Centre for Neuroimaging, London, United Kingdom; http://www.fil.ion.ucl.ac.uk/spm/), and the FMRIB Software Library (FSL, FMRIB, Oxford, United Kingdom; http://fsl.fmrib.ox.ac.uk/fsl/fslwiki/) software packages. DSC and iVASO images were motion corrected for head movement between scans. Anatomical (MPRAGE and FLAIR) and iVASO images were all co-registered to DSC images for each subject. Image segmentation was performed on MPRAGE images to obtain gray matter (GM) and white matter (WM) masks. Subsequently, DSC images were analyzed using a plugin toolbox DSCoMAN in the ImageJ software (http://imagej.nih.gov/ij/index.html). Maps of CBV and MTT were generated. The iVASO images were analyzed with in-house routines programmed in Matlab (MathWorks, Natick, MA, USA). The difference signal between the nulling and control iVASO images were calculated using the surround subtraction method, and CBVa and ATT maps were fitted numerically from the difference signals according to the iVASO equations (18). The skull was excluded during numerical fitting.

Region-of-interest (ROI) analysis was conducted on the DSC and iVASO data. ROIs of tumoral regions and similar-sized contralateral normal appearing GM regions were carefully selected on the anatomical images (MPRAGE and FLAIR, after co-registration to DSC and iVASO images) for each patient, and then projected onto the DSC and iVASO images. In the contralateral regions, only voxels from the GM masks were included. The same ROIs were used for both DSC and iVASO analysis for each patient. The ROI selection was performed by a neuroradiolo-gist (Y.W.) with more than 10 years of related experience. Efforts were made to avoid necrotic and cystic regions and major macrovessels in the brain. While contralateral WM is a more common choice for internal reference region (5,8,44,45), contralateral GM was adopted here mainly because cortical GM was involved in the tumoral regions of most patients recruited for this study. Average CBV and MTT from DSC, and CBVa and ATT from iVASO were calculated for each ROI. Signal-to-noise ratio (SNR) was calculated on the original DSC images and iVASO difference images in each ROI, and contrast-to-noise ratio (CNR) between tumoral and contralateral regions was taken as the product of SNR and relative changes in respective parameters.

Statistical analysis

Paired t-tests were performed to examine group difference in the perfusion parameters between tumoral and contralateral ROIs, and to compare SNR and CNR between DSC and iVASO MRI. Effect size was estimated with Cohen's d. To reduce the influence from differences in individual baseline physiological status and age differences, we calculated the

ratio of tumor/contralateral for each parameter, which was used in subsequent correlation analysis. Correlations between these parameters and WHO tumor grade were assessed using two methods: 1) the adjusted R^2 from linear regression with subject age included as an independent variable; 2) the Spearman's rank correlation (ρ) given subject age as a third variable. Compared to linear regression, the Spearman's rank correlation examines the monotonic relationship between two variables and is more suitable for ordinal variables with a limited number of levels such as the WHO tumor grade (46). Correlations between DSC CBV and iVASO CBVa, and between DSC MTT and iVASO ATT were assessed using linear regression. Multiple comparisons were corrected with the false discovery rate.

Results

Figure 1 demonstrates anatomical, DSC and iVASO images from patient 14 (female, 21 years old, WHO grade II oligodendroglioma in the left frontal lobe). Images after co-registration were shown, and ROI selection in the tumoral and contralateral regions were illustrated. Note that the contralateral ROIs were made slightly larger than the tumor ROIs, but only voxels from the GM masks in the contralateral regions were included for signal average. Thus, the total number of voxels were approximately the same between tumoral and contralateral ROIs. In this WHO II case, DSC CBV and iVASO CBVa in the tumoral region were both higher than contra-lateral WM, but lower than contralateral GM, which is typical in low grade brain tumors. DSC MTT was comparable between tumoral and contralateral regions, while iVASO ATT was shorter in the tumor. Note that ATT in *normal* WM can be longer than iVASO TIs used in the current protocol (18,47). In such voxels, ATT cannot be determined by the numerical fitting procedure with the data acquired at these TIs and therefore is set to zero in the ATT map (more discussion on this later).

DSC and iVASO MRI measures (mean values from the ROIs) in twelve patients are listed in Table 1 and statistical results for each WHO tumor grade are summarized in Table 2. DSC CBV values in tumoral regions were all higher compared to contralateral regions in WHO grade IV patients (but not statistically significant, $P = 0.21$, effect size = 1.74), but were comparable in WHO grade II and III patients. DSC MTT values were comparable between tumoral and contralateral regions in all patients. The iVASO CBVa values were significantly lower in tumoral regions in WHO grade II patients ($P < 0.03$, effect size = −1.71). No significant differences were found in CBVa between WHO III tumors and contralateral normal appearing tissue. Among the three WHO grade III patients, the oligodendroglioma case (case 1) showed greater tumor CBVa than contralateral hemispheric CBVa, whereas both anaplastic astrocytoma cases (cases 4 and 5) showed lower CBVa in tumoral regions than in contralateral hemispheric regions. CBVa values in all three WHO grade IV patients were greater in tumoral than in contralateral regions ($P = 0.001$, effect size = 1.49). The iVASO ATT values were all shorter in tumoral ROIs compared to contralateral regions except for case 1 (Table 1, statistics in Table 2).

From correlation analysis, the iVASO CBVa ratio showed the strongest positive correlation with WHO tumor grade ($\rho = 0.37$, $P = 0.04$; $R^2 = 0.68$, $P = 0.001$, Figure 2b). The DSC CBV ratio showed a trend of correlation with WHO tumor grade ($\rho = 0.28$, $P = 0.5$; $R^2 = 0.21$, $P = 0.1$, Figure 2a). Neither DSC MTT ratio nor iVASO ATT ratio showed significant

association with WHO tumor grade in our data (Figures 2c,d). Subject age showed negligible contribution in all correlations analyzed above (Figure 2). Both DSC CBV and iVASO CBVa values from the tumoral ROIs before normalization by contralateral values showed similar results but slightly weaker correlations with WHO tumor grade than the corresponding ratios of tumor/contralateral tissue. No correlation with WHO tumor grade was observed from contralateral values.

SNR was comparable between DSC and iVASO images in all three groups (Table 2; WHO II tumor: P = 0.98, 95% confidence interval or C.I. = (−7.54, 7.41); WHO II contralateral: P = 0.89, C.I. = (−6.29, 5.64); WHO III tumor: P = 0.32, C.I. = (−11.44, 6.04); WHO III contralateral: P = 0.89, C.I. = (−21.78, 23.42); WHO IV tumor: P = 0.92, C.I. = (−14.11, 13.37); WHO IV contralateral: P = 0.38, C.I. = (−20.38, 11.91)). As the relative changes between tumoral and contralateral regions were greater in iVASO CBVa than in DSC CBV in WHO II and III patients, CNR of iVASO CBVa was also significantly higher in these groups (WHO II: P = 0.004, C.I. = (−8.53, −2.71); WHO III: P = 0.04, C.I. = (−7.73, −0.59)). Relative changes and CNR were comparable (P = 0.94, C.I. = (−6.55, 6.83)) between DSC CBV and iVASO CBVa in WHO IV patients. Figure 3 demonstrates the correlations between corresponding DSC and iVASO measures. A trend of positive correlation between DSC CBV ratio and iVASO CBVa ratio was observed in our data (R^2 = 0.28, P = 0.07, Figure 3a). No correlation was found between DSC MTT ratio and iVASO ATT ratio (Figure 3b).

Discussion

In this study, we investigated the potential diagnostic value of CBVa measured by the recently developed iVASO MRI approach for the assessment of cerebral perfusion in 12 brain tumor patients. Absolute cerebral blood volume of pial arteries and arterioles (CBVa) in physiological units (ml blood/100 ml brain tissue) was measured using iVASO MRI in brain tumor and similar-sized contralateral hemispheric areas in each patient. The results were compared with total CBV measured by DSC MRI as the current standard perfusion MRI protocol in brain tumor patients. DSC CBV and iVASO CBVa values in normal appearing tissue from the contralateral ROIs were all within the range of normal values reported in the literature (18,23,48), providing some validation for our results. In our data, CBVa values measured with iVASO MRI in tumoral regions demonstrated a stronger positive correlation with WHO tumor grade than CBV values measured with DSC MRI in the same patients, suggesting a better sensitivity for CBVa than total CBV for probing tumor perfusion. The iVASO approach does not require the injection of exogenous contrast media. This may be a potential advantage for clinical applications compared to DSC MRI considering the extra time and cost needed for contrast administration, possible risk of adverse contrast reactions, and the known side effects associated with the commonly used Gadolinium based contrast agents. The actual scan time of DSC MRI is usually several minutes shorter than iVASO MRI. However, the administration of contrast media in patients makes the total duration needed for DSC scans comparable or even longer than iVASO MRI.

Tissue perfusion, commonly measured by CBV and/or CBF, is one of the key physiological parameters for the evaluation of tumor viability (4). There is evidence showing that

angiogenesis (and resultant CBV increase) may occur before any increase in CBF (38). Particularly in tumors, several studies have demonstrated that CBV changes may precede CBF changes (6), and that CBV may be a more proximal and sensitive measure of metabolic perturbations in the tissue (7). DSC MRI has been routinely used to assess tissue perfusion in tumor patients. In our data, despite the relatively small sample size, DSC CBV ratios (tumor/contralateral) showed a trend of correlation with WHO tumor grade. Particularly, all WHO grade IV patients had higher tumor CBV compared to contralateral normal appearing GM regions. These results are consistent with a number of reports in the literature using DSC MRI in brain tumor patients (1,5,10-12).

As small arterial and arteriolar vessels are the most actively regulated blood vessels in the microvasculature, any disturbance in tissue metabolism may have more direct effects on these arterial vessels than on venous vessels (35-37). While total CBV (sum of arterial, capillary and venous vessels) is measured in DSC MRI, the blood volume of small arteries and arterioles in tissue is measured separately from the rest of the microvasculature in iVASO MRI. Interestingly, in our data, iVASO CBVa values demonstrated a stronger correlation with WHO tumor grade than DSC CBV values in the same patients. Also, the average difference between WHO grades II and III oligodendrogliomas was greater in iVASO CBVa than in DSC CBV. This seems to imply that changes in CBVa in brain tumors might be a better classifier than changes in the total microvasculature for the stratification of brain tumors, especially between WHO grades II and III. This finding may be of potential diagnostic value since differences between grade II and IV tumors is usually evident on contrast-enhanced structural MRI and DSC perfusion images, while differentiation between grade II and III tumors is often more difficult. Further investigation with a large cohort is required to establish such an effect.

Interestingly, the two cases with WHO grade III anaplastic astrocytoma showed both lower DSC CBV and lower iVASO CBVa than contralateral GM regions. Anaplastic astrocytoma is a rare type of malignant astrocytoma that is classified as WHO grade III. Pathologic evaluation shows that anaplastic astrocytomas are similar to WHO grade II tumors, but are more cellular. The vascular proliferation typically seen in high grade (WHO grades III or IV) tumors may be absent in some anaplastic astrocytomas (1,49), which would explain the lower CBV and CBVa values observed in our data. Further investigation is merited to confirm our findings with a sufficient sample size and to further characterize the perfusion abnormalities in this type of brain tumor.

The MTT value measured in DSC MRI is defined as the average time for the injected contrast agent to traverse the entire microvasculature. Our data showed comparable MTT values in tumoral and contralateral regions, and no significant correlation with WHO tumor grade was found. This is in line with some reports in the literature (1,3,5). The ATT value measured in iVASO MRI reflects the time it takes for inverted blood water spins to perfuse the arterial compartment of the microvasculature before reaching the capillary bed. The ATT values in the contralateral normal appearing GM regions measured in this study were slightly shorter than the values reported in our previous studies in healthy volunteers using the same method (18). We attribute this mainly to the fact that ATT can vary substantially between different brain regions (50,51). The values in our previous studies for technology

development were measured in a relatively distal location in the cortex (18), which usually has longer vascular transit times (50,51). In our data, 11 out of the 12 brain tumor patients showed shorter ATT values in tumor compared to contralateral GM regions, which seems to imply that pial arteries and arterioles are short in these brain tumors. The fact that ATT, but not MTT, reduced in tumoral regions may indicate longer transit times in the capillaries and venous vessels, which would align with the trend of increased CBV measured by DSC. The one case (case 1, WHO grade III oligodendroglioma) that had longer tumor ATT also showed substantially larger CBVa in tumoral region, which could implicate a largely expanded arteriolar network leading to prolonged ATT values in this tumor patient. No significant correlation between ATT and WHO tumor grade was found. These results imply that vascular transit times alone may not be sufficient to characterize the vascular networks in tumors of different WHO grades.

We found a trend of association between DSC CBV and iVASO CBVa, but no association between DSC MTT and iVASO ATT. This can be anticipated since the underlying physiological information that these parameters measure is distinct from each other, as discussed above. SNR was comparable between DSC and iVASO images with the imaging parameters used in this study, whereas CNR was greater in iVASO CBVa than DSC CBV in WHO II and III patients but comparable in WHO IV patients. However, better SNR can be attained by adjusting imaging parameters such as voxel size, TE, number of signal averages and others. For instance, as the DSC signal mainly originates from the magnetic susceptibility effects of contrast media, it requires a relatively long TE to get the optimal effect, whereas iVASO can use the shortest TE possible, furnishing a higher MR signal and thus better SNR. On the other hand, as the iVASO signal is calculated from the subtraction of consecutive nulling and control scans, it is more sensitive to noises from subject motion and physiological fluctuations. Nevertheless, we would like to note that our main finding in the present study (stronger correlation between CBVa and WHO grade) is more likely due to the specificity of underlying physiological information measured by these two methods (CBVa in iVASO, and total CBV in DSC), rather than SNR discrepancies. As CBVa accounts for about 20% of total CBV in the brain (52), the DSC measures may have dominant contributions from the capillaries and venous vessels.

Arterial blood volume can also be measured with ASL MRI by comparing scans with and without crushing gradients (53). The main difference is that ASL and iVASO measure the arterial blood volume *above* and *below* certain velocity threshold, respectively (18,53), which reflect two different aspects of the arterial vasculature. Another ASL based approach is to employ a two-stage model to analyze multi-TI ASL data for arterial blood volume estimation, which also includes substantial contribution from large arteries (54). It has been shown that ASL based arterial blood volume correlated with DSC CBV in brain tumors and increased with tumor grade (53,54), generally consistent with our results. Many other methods have been developed for CBVa measurement. The readers are referred to a more comprehensive discussion on existing CBVa methods in our previous technology development papers (18,19). As the current paper is intended to be an initial report and assessment of the application of iVASO MRI in brain tumor patients, we only included CBVa studies relevant to brain tumor imaging in the discussion above.

The absolute values of blood volume and vascular transit times can vary substantially depending on various factors such as age, sex, and especially brain region, as can be seen in the average values from the contralateral ROIs in our data. To mitigate the influence from these variations, parameter values from tumoral ROIs were normalized by contralateral values from the same subject and the ratio between tumoral and contralateral regions was then used as the primary outcome measure in the correlation analysis. Indeed, the normalized quantities showed stronger correlations with WHO tumor grade in our data. Various cortical and sub-cortical regions have been suggested as internal references, such as contralateral WM or GM areas, mirror region that includes both WM and GM, the cerebellum and thalamus (5,8,44,45). Here, we chose to use contralateral GM as the internal reference region for normalization, mainly because the lesions in the majority of our cases involved cortical GM regions. As CBV and CBVa values in GM are usually higher than those in WM in normal brains (10,18,48), low grade (WHO II or III) glioma can sometimes have comparable or lower CBV and CBVa values than contralateral GM, as seen in our data as well as reported in the literature (5). Nevertheless, as the same ROIs were used in both DSC and iVASO analysis, this should not affect the comparison of these two methods. Also, the choice of contralateral region should have negligible effect on the correlations between perfusion measures and WHO tumor grade (our main findings in the current study).

In this study, all iVASO scans were performed at 7T as part of a research session while the DSC scans were acquired at 3T as part of the clinical protocol in the same patients. The iVASO approach was originally developed at 3T and the total scan time is identical at both field strengths (18). In iVASO, the physiological parameters (CBVa and ATT) are derived from the difference signals between two scans with and without arterial blood nulling. Because the SNR of the difference signal is dominated by physiological noise which generally increases with field strength, we anticipate similar results from iVASO MRI performed on 3T clinical scanners (lower physiological noise than 7T). Our SNR measurements in iVASO in the current study at 7T indeed showed comparable results to our previous study using similar imaging parameters (voxel size, TE, and total scan time etc.) at 3T (18). A matched comparison between DSC and iVASO MRI at 3T is required to further confirm this expectation.

Several confounding factors in this study should be discussed. First, cerebral perfusion can alter markedly with age, and in our sample, the average age of WHO grade IV patients was significantly greater than the other two groups. Therefore, in addition to the normalization with contralateral values, we also included age as an independent variable in the correlation analysis. Our results demonstrated that age had a negligible effect on the correlations detected between the perfusion parameters and WHO tumor grade in our data, especially when the ratios of tumoral and contralateral values were used. Secondly, the presence of large macrovessels and necrotic zones could significantly alter the perfusion parameters in our measurements, which does not reflect microvascular information in tumor and brain tissues, and thus results in misleading values. We therefore took extra care when selecting ROIs to ensure the exclusion of these regions in our analysis.

Some limitations of this pilot study should be noted. First, despite some statistically significant results in our data, the overall sample size is relatively small. Follow-up studies

with a larger cohort of brain tumor patients are warranted to validate the current findings. Our results can serve as the basis for power analysis in future studies. The second limitation is the single slice spatial coverage in our iVASO data. When the study was performed, the iVASO MRI technique had just been developed and a single slice version was adopted. The slice was carefully placed on each patient through the tumoral regions to capture the most cellular portions of the tumors and to exclude necrotic areas (based on anatomical and DSC perfusion images). We have recently developed a 3D iVASO MRI pulse sequence at both 3T and 7T (55), which is capable of acquiring whole brain CBVa maps with the same total scan time as in single slice iVASO MRI used here. We will use 3D iVASO MRI in our follow-up studies to evaluate CBVa changes in the entire tumor and potential heterogeneities among different sub-regions in tumors. A whole brain coverage will also allow the use of regions such as the thalamus and cerebellum (5,8,44,45) as the internal reference for normalization in order to reduce inter-subject variability. Finally, similar to ASL MRI, the sensitivity of iVASO MRI in *normal* WM regions diminishes mainly due to a much longer ATT in WM (> 2 s) (47), as the longest possible blood nulling TI in iVASO is approximately 1.8 s (determined by blood T1 and imaging parameters such as TR). However, this limitation only applies to *normal* WM. In WM regions in brain tumors and normal GM, perfusion is elevated compared to normal WM and typical ATTs are well below 1.5 s (not MTT) (51,54), which is in the optimal range of TIs for iVASO MRI with the current imaging parameters (18). For brain tissue with an exceedingly long ATT, it is possible to use a TI beyond blood nulling point and an adjusted iVASO theory to calculate CBVa values.

In conclusion, we demonstrated the potential clinical value of an important perfusion parameter, arteriolar cerebral blood volume (CBVa), measured by a newly developed iVASO MRI technique in brain tumor patients without exogenous contrast agent administration. Our results showed a trend of correlation between iVASO CBVa and the current standard DSC CBV values. Moreover, iVASO CBVa showed a stronger correlation with WHO tumor grade than DSC CBV measured in the same patients. Further investigation is warranted to validate our findings in a larger cohort and to determine whether CBVa could be employed as a useful biomarker for the assessment of biologic aggressiveness of brain tumors and potential responses to antiangiogenic therapies.

Acknowledgments

The authors thank Mr. Joseph S. Gillen, Ms. Terri Lee Brawner, Ms. Kathleen A. Kahl and Ms. Ivana Kusevic for experimental assistance. This project was supported by the Johns Hopkins University Brain Science Institute grant and the National Institute of Biomedical Imaging and Bioengineering of the National Institutes of Health through resource grant P41 EB015909. Dr. Jun Hua's salary is paid in part from a grant to the Kennedy Krieger Institute from Philips Healthcare. Equipment used in the study is manufactured by Philips. Dr. van Zijl is a paid lecturer for Philips Healthcare. This arrangement has been approved by Johns Hopkins University in accordance with its conflict of interest policies.

References

1. Cha S, Tihan T, Crawford F, et al. Differentiation of low-grade oligodendrogliomas from low-gradeastrocytomas by using quantitative blood-volume measurements derived from dynamic susceptibility contrast enhanced MR imaging. Am J Neuroradiol. 2005; 26(2):266–273. [PubMed: 15709123]

2. Lu H, Pollack E, Young R, et al. Predicting Grade of Cerebral Glioma Using Vascular-Space Occupancy MR Imaging. AJNR Am J Neuroradiol. 2008; 29(2):373. [PubMed: 17974612]
3. Jain RK. Determinants of tumor blood flow: a review. Cancer research. 1988; 48(10):2641–2658. [PubMed: 3282647]
4. Folkman J. Angiogenesis in cancer, vascular, rheumatoid and other disease. Nat Med. 1995; 1(1): 27–31. [PubMed: 7584949]
5. Romano A, Rossi Espagnet MC, Calabria LF, et al. Clinical applications of dynamic susceptibility contrast perfusion-weighted MR imaging in brain tumours. La Radiologia medica. 2012; 117(3): 445–460. [PubMed: 21892719]
6. Oku T, Tjuvajev JG, Miyagawa T, et al. Tumor growth modulation by sense and antisense vascular endothelial growth factor gene expression: effects on angiogenesis, vascular permeability, blood volume, blood flow, fluorodeoxyglucose uptake, and proliferation of human melanoma intracerebral xenografts. Cancer research. 1998; 58(18):4185–4192. [PubMed: 9751633]
7. Aronen HJ, Pardo FS, Kennedy DN, et al. High microvascular blood volume is associated with high glucose uptake and tumor angiogenesis in human gliomas. Clin Cancer Res. 2000; 6(6):2189–2200. [PubMed: 10873068]
8. Cha S, Knopp EA, Johnson G, Wetzel SG, Litt AW, Zagzag D. Intracranial mass lesions: dynamic contrast-enhanced susceptibility-weighted echo-planar perfusion MR imaging. Radiology. 2002; 223(1):11–29. [PubMed: 11930044]
9. Knutsson L, Stahlberg F, Wirestam R. Absolute quantification of perfusion using dynamic susceptibility contrast MRI: pitfalls and possibilities. MAGMA. 2010; 23(1):1–21. [PubMed: 19960361]
10. Aronen HJ, Gazit IE, Louis DN, et al. Cerebral blood volume maps of gliomas: Comparison with tumor grade and histologic findings. Radiology. 1994; 191:41–51. [PubMed: 8134596]
11. Knopp EA, Cha S, Johnson G, et al. Glial neoplasms: Dynamic contrast-enhanced T2*-weighted MR imaging. Radiology. 1999; 211(3):791–798. [PubMed: 10352608]
12. Law M, Yang S, Babb JS, et al. Comparison of cerebral blood volume and vascular permeability from dynamic susceptibility contrast-enhanced perfusion MR imaging with glioma grade. Am J Neuroradiol. 2004; 25:746–755. [PubMed: 15140713]
13. Grobner T. Gadolinium--a specific trigger for the development of nephrogenic fibrosing dermopathy and nephrogenic systemic fibrosis? Nephrology, dialysis, transplantation : official publication of the European Dialysis and Transplant Association - European Renal Association. 2006; 21(4):1104–1108.
14. Marckmann P, Skov L, Rossen K, et al. Nephrogenic systemic fibrosis: suspected causative role of gadodiamide used for contrast-enhanced magnetic resonance imaging. Journal of the American Society of Nephrology : JASN. 2006; 17(9):2359–2362. [PubMed: 16885403]
15. McDonald RJ, McDonald JS, Kallmes DF, et al. Intracranial Gadolinium Deposition after Contrast-enhanced MR Imaging. Radiology. 2015; 275(3):772–782. [PubMed: 25742194]
16. Fujima N, Kudo K, Tsukahara A, et al. Measurement of tumor blood flow in head and neck squamous cell carcinoma by pseudo-continuous arterial spin labeling: comparison with dynamic contrast-enhanced MRI. J Magn Reson Imaging. 2015; 41(4):983–991.
17. Truong MT, Saito N, Ozonoff A, et al. Prediction of locoregional control in head and neck squamous cell carcinoma with serial CT perfusion during radiotherapy. AJNR Am J Neuroradiol. 2011; 32(7):1195–1201. [PubMed: 21757530]
18. Hua J, Qin Q, Pekar JJ, Zijl PC. Measurement of absolute arterial cerebral blood volume in human brain without using a contrast agent. NMR Biomed. 2011; 24(10):1313–1325. [PubMed: 21608057]
19. Hua J, Qin Q, Donahue MJ, Zhou J, Pekar JJ, van Zijl PC. Inflow-based vascular-space-occupancy (iVASO) MRI. Magn Reson Med. 2011; 66(1):40–56. [PubMed: 21695719]
20. Donahue MJ, Sideso E, MacIntosh BJ, Kennedy J, Handa A, Jezzard P. Absolute arterial cerebral blood volume quantification using inflow vascular-space-occupancy with dynamic subtraction magnetic resonance imaging. J Cereb Blood Flow Metab. 2010; 30(7):1329–1342. [PubMed: 20145656]

21. Donahue, MJ.; MacIntosh, BJ.; Sideso, E., et al. Absolute cerebral blood volume (CBV) quantification without contrast agents using inflow vascular-space-occupancy (iVASO) with dynamic subtraction.. Proc 17th Annual Meeting ISMRM; Hawaii, USA. 2009; p. 628
22. Hua, J.; Qin, Q.; Pekar, J.; van Zijl, PCM. Measuring Absolute Arteriolar Cerebral Blood Volume (CBVa) in Human Brain Gray Matter (GM) without Contrast Agent.. Proc 17th Annual Meeting ISMRM; Hawaii, USA. 2009; p. 5314
23. Hua J, Unschuld PG, Margolis RL, van Zijl PC, Ross CA. Elevated arteriolar cerebral blood volume in prodromal Huntington's disease. Mov Disord. 2014; 29(3):396–401. [PubMed: 23847161]
24. Rane S, Talati P, Donahue MJ, Heckers S. Inflow-vascular space occupancy (iVASO) reproducibility in the hippocampus and cortex at different blood water nulling times. Magn Reson Med. 2015
25. Helpern JA, Branch CA, Yongbi MN, Huang NC. Perfusion imaging by un-inverted flow-sensitive alternating inversion recovery (UNFAIR). Magn Reson Imaging. 1997; 15(2):135. [PubMed: 9106140]
26. Tanabe JL, Yongbi M, Branch C, Hrabe J, Johnson G, Helpern JA. MR perfusion imaging in human brain using the UNFAIR technique. Un-inverted flow-sensitive alternating inversion recovery. J Magn Reson Imaging. 1999; 9(6):761. [PubMed: 10373023]
27. Berr SS, Mai VM. Extraslice spin tagging (EST) magnetic resonance imaging for the determination of perfusion. J Magn Reson Imaging. 1999; 9(1):146. [PubMed: 10030662]
28. Jahng GH, Weiner MW, Schuff N. Improved arterial spin labeling method: applications for measurements of cerebral blood flow in human brain at high magnetic field MRI. Med Phys. 2007; 34(11):4519. [PubMed: 18072518]
29. Alsop DC, Detre JA. Reduced transit-time sensitivity in noninvasive magnetic resonance imaging of human cerebral blood flow. J Cereb Blood Flow Metab. 1996; 16(6):1236. [PubMed: 8898697]
30. Wong EC, Buxton RB, Frank LR. Quantitative imaging of perfusion using a single subtraction (QUIPSS and QUIPSS II). Magn Reson Med. 1998; 39(5):702–708. [PubMed: 9581600]
31. Ye FQ, Mattay VS, Jezzard P, Frank JA, Weinberger DR, McLaughlin AC. Correction for vascular artifacts in cerebral blood flow values measured by using arterial spin tagging techniques. Magn Reson Med. 1997; 37(2):226. [PubMed: 9001147]
32. Zhao JM, Clingman CS, Narvainen MJ, Kauppinen RA, van Zijl PC. Oxygenation and hematocrit dependence of transverse relaxation rates of blood at 3T. Magn Reson Med. 2007; 58(3):592. [PubMed: 17763354]
33. Hillman EM, Devor A, Bouchard MB, et al. Depth-resolved optical imaging and microscopy of vascular compartment dynamics during somatosensory stimulation. Neuroimage. 2007; 35(1):89. [PubMed: 17222567]
34. Vanzetta I, Hildesheim R, Grinvald A. Compartment-resolved imaging of activity-dependent dynamics of cortical blood volume and oximetry. J Neurosci. 2005; 25(9):2233. [PubMed: 15745949]
35. Iadecola C, Nedergaard M. Glial regulation of the cerebral microvasculature. Nat Neurosci. 2007; 10(11):1369–1376. [PubMed: 17965657]
36. Ito H, Ibaraki M, Kanno I, Fukuda H, Miura S. Changes in the arterial fraction of human cerebral blood volume during hypercapnia and hypocapnia measured by positron emission tomography. J Cereb Blood Flow Metab. 2005; 25(7):852. [PubMed: 15716851]
37. Kim T, Hendrich KS, Masamoto K, Kim SG. Arterial versus total blood volume changes during neural activity-induced cerebral blood flow change: implication for BOLD fMRI. J Cereb Blood Flow Metab. 2007; 27(6):1235. [PubMed: 17180136]
38. Hansen-Smith F, Egginton S, Zhou AL, Hudlicka O. Growth of arterioles precedes that of capillaries in stretch-induced angiogenesis in skeletal muscle. Microvascular research. 2001; 62(1): 1–14. [PubMed: 11421656]
39. Haines K, Smith NB, Webb AG. New high dielectric constant materials for tailoring the B1+ distribution at high magnetic fields. J Magn Reson. 2010; 203(2):323–327. [PubMed: 20122862]

40. Teeuwisse WM, Brink WM, Webb AG. Quantitative assessment of the effects of high-permittivity pads in 7 Tesla MRI of the brain. Magn Reson Med. 2012; 67(5):1285–1293. [PubMed: 21826732]
41. Hua J, Jones CK, Qin Q, van Zijl PC. Implementation of vascular-space-occupancy MRI at 7T. Magn Reson Med. 2013; 69(4):1003–1013. [PubMed: 22585570]
42. Bouvy WH, Geurts LJ, Kuijf HJ, et al. Assessment of blood flow velocity and pulsatility in cerebral perforating arteries with 7-T quantitative flow MRI. NMR Biomed. 2015
43. Kobari M, Gotoh F, Fukuuchi Y, Tanaka K, Suzuki N, Uematsu D. Blood flow velocity in the pial arteries of cats, with particular reference to the vessel diameter. J Cereb Blood Flow Metab. 1984; 4(1):110–114. [PubMed: 6693510]
44. Jiang J, Zhao L, Zhang Y, et al. Comparative analysis of arterial spin labeling and dynamic susceptibility contrast perfusion imaging for quantitative perfusion measurements of brain tumors. Int J Clin Exp Pathol. 2014; 7(6):2790–2799. [PubMed: 25031698]
45. Lev MH, Ozsunar Y, Henson JW, et al. Glial tumor grading and outcome prediction using dynamic spin-echo MR susceptibility mapping compared with conventional contrast-enhanced MR: confounding effect of elevated rCBV of oligodendrogliomas [corrected]. AJNR Am J Neuroradiol. 2004; 25(2):214–221. [PubMed: 14970020]
46. Rosner, B. Fundamentals of Biostatistics. Brooks/Cole; Boston, MA, USA: p. 2011
47. van Osch MJ, Teeuwisse WM, van Walderveen MA, Hendrikse J, Kies DA, van Buchem MA. Can arterial spin labeling detect white matter perfusion signal? Magn Reson Med. 2009; 62(1):165–173. [PubMed: 19365865]
48. Vonken EP, van Osch MJ, Willems PW, et al. Repeated quantitative perfusion and contrast permeability measurement in the MRI examination of a CNS tumor. Eur Radiol. 2000; 10(9): 1447–1451. [PubMed: 10997434]
49. Compostella A, Tosoni A, Blatt V, Franceschi E, Brandes AA. Prognostic factors for anaplastic astrocytomas. Journal of neuro-oncology. 2007; 81(3):295–303. [PubMed: 17001519]
50. Gonzalez-At JB, Alsop DC, Detre JA. Cerebral perfusion and arterial transit time changes during task activation determined with continuous arterial spin labeling. Magn Reson Med. 2000; 43(5): 739. [PubMed: 10800040]
51. Hendrikse J, Petersen ET, van Laar PJ, Golay X. Cerebral border zones between distal end branches of intracranial arteries: MR imaging. Radiology. 2008; 246(2):572. [PubMed: 18055872]
52. van Zijl PC, Eleff SM, Ulatowski JA, et al. Quantitative assessment of blood flow, blood volume and blood oxygenation effects in functional magnetic resonance imaging. Nat Med. 1998; 4(2): 159. [PubMed: 9461188]
53. van Westen D, Petersen ET, Wirestam R, et al. Correlation between arterial blood volume obtained by arterial spin labelling and cerebral blood volume in intracranial tumours. MAGMA. 2011; 24(4):211–223. [PubMed: 21594585]
54. Hales PW, Phipps KP, Kaur R, Clark CA. A two-stage model for in vivo assessment of brain tumor perfusion and abnormal vascular structure using arterial spin labeling. PLoS One. 2013; 8(10):e75717. [PubMed: 24098395]
55. Hua, J.; Lee, S.; Blair, NIS., et al. Reduced Grey Matter Arteriolar Cerebral Blood Volume in Schizophrenia.. Proc 23rd Annual Meeting ISMRM; Toronto, Canada. 2015;

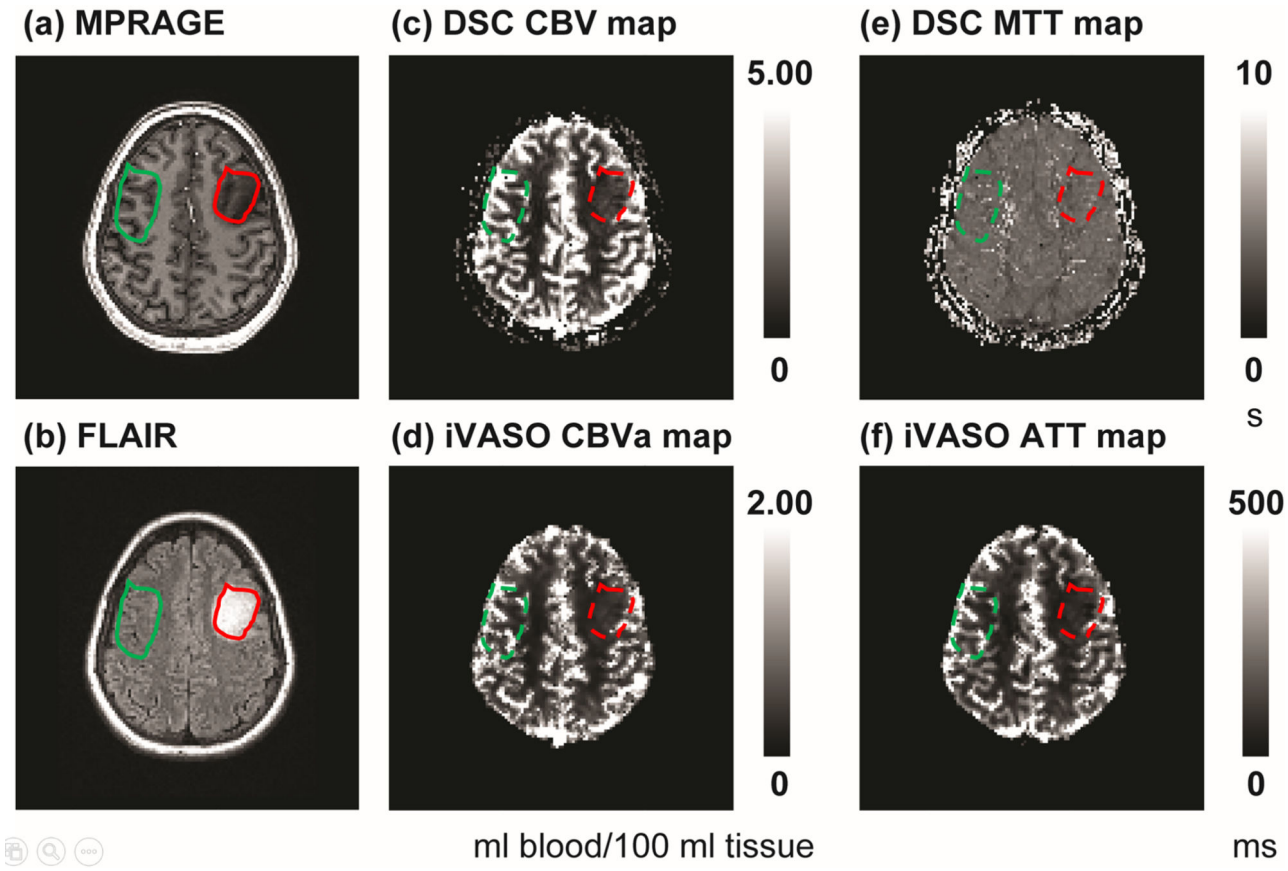

Figure 1.

Images from patient 14 (female, 21 years old, WHO grade II oligodendroglioma in the left frontal lobe). (a) MPRAGE, (b) FLAIR, (c) DSC CBV map, (d) iVASO CBVa map, (e) DSC MTT map, and (f) iVASO ATT map. Units: ml blood/100 ml tissue for CBV and CBVa, second (s) for MTT, and millisecond (ms) for ATT. Images after co-registration are shown. ROIs in the tumor (red) and contralateral (green) regions were first selected on MPRAGE and FLAIR images (solid line), and then projected onto DSC and iVASO images (dashed line). The contralateral ROIs were made slightly larger than the tumor ROIs, but only voxels from the GM masks in the contralateral regions were included for signal average. Thus, the total number of voxels were approximately the same between tumoral and contralateral ROIs. In iVASO images, the skull was excluded during the calculation of CBVa and ATT maps.

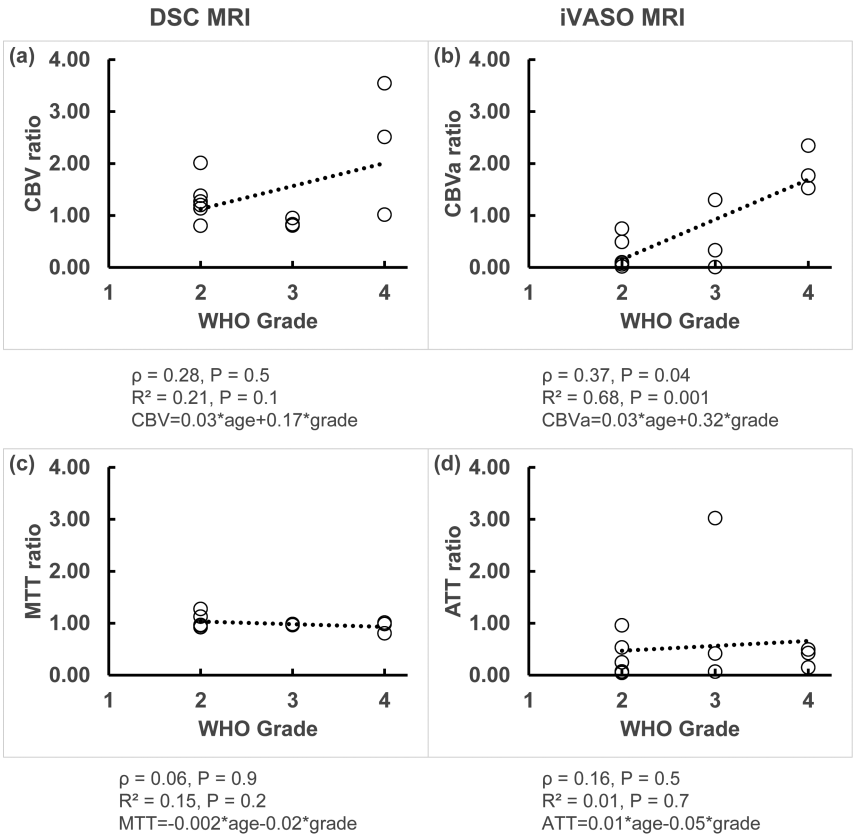

Figure 2.

Correlation analysis between the DSC and iVASO measures (ratio of tumor/contralateral) with WHO tumor grade. The open circles represent data points, and the trend lines from linear regression are shown with dotted lines. Spearman's rank correlation coefficient (ρ), adjusted R^2 and the fitted equation from multiple regression, and P values are shown under each graph.

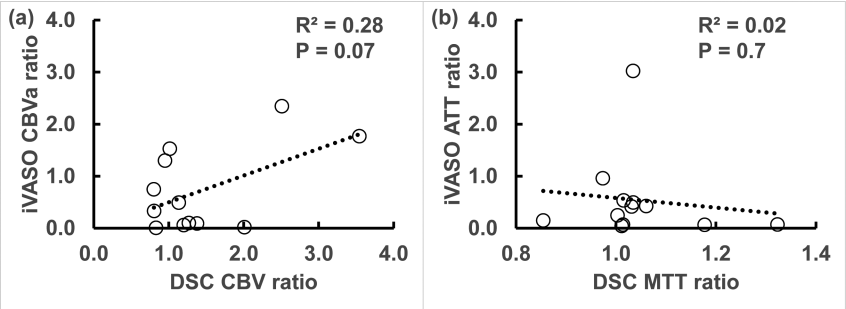

Figure 3.

Correlation analysis between corresponding iVASO and DSC measures (ratio of tumor/contralateral). The open circles represent data points, and the trend lines from linear regression are shown with dotted lines. Adjusted R^2 and P value are shown on each graph.

Table 1

Demographic data and perfusion measurements (mean values from ROI) in tumor patients (sorted by WHO tumor grade).

Pt. No.	Sex	Age	Tumor Location	Histology	WHO Grade	DSC MRI						iVASO MRI					
						CBV (ml/100 ml)			MTT (s)			CBVa (ml/100 ml)			ATT (ms)		
						tumor	contra*	t/c*	tumor	contra	t/c	tumor	contra	t/c	tumor	contra	t/c
3	M	23	Right frontal	Oligodendroglioma	II	2.21	1.84	1.20	4.80	4.25	1.13	0.02	0.34	0.06	31.20	490.75	0.06
6	M	36	Right perirolandic	Oligoastrocytoma	II	4.07	3.59	1.13	4.18	4.53	0.92	0.51	1.04	0.49	222.13	231.31	0.96
11	M	23	Left perirolandic	Low grade glioma	II	2.36	1.86	1.27	6.24	4.90	1.27	0.04	0.41	0.10	30.48	431.41	0.07
12	M	44	Left frontal	Oligodendroglioma	II	4.50	2.24	2.01	4.97	5.17	0.96	0.03	1.59	0.02	22.90	544.38	0.04
13	M	23	Left perirolandic	Oligodendroglioma	II	3.79	2.75	1.38	4.84	5.07	0.95	0.13	1.44	0.09	98.71	399.35	0.25
14	F	21	Left frontal	Oligodendroglioma	II	2.76	3.45	0.80	5.42	5.62	0.97	0.74	0.99	0.75	216.54	406.49	0.53
1	M	44	Left frontal	Oligodendroglioma	III	5.99	6.29	0.95	6.71	6.82	0.98	1.74	1.34	1.30	770.05	254.75	3.02
4	M	29	Left parietooccipital	Anaplastic astrocytoma	III	4.71	5.84	0.81	4.97	5.06	0.98	0.41	1.24	0.33	191.70	458.82	0.42
5	M	22	Right occipital	Anaplastic astrocytoma	III	2.40	2.89	0.83	4.95	5.13	0.96	0.01	1.32	0.01	21.01	308.11	0.07
7	F	62	Left frontal	Glioblastoma	IV	6.31	1.78	3.54	4.58	4.65	0.98	0.99	0.56	1.77	253.47	514.70	0.49
8	M	65	Right temporal	Glioblastoma	IV	4.15	4.09	1.01	3.79	4.71	0.80	1.36	0.89	1.53	117.00	785.28	0.15
10	F	69	Right frontal	Glioblastoma	IV	4.01	1.60	2.51	5.28	5.23	1.01	0.75	0.32	2.34	149.55	351.76	0.43

*contra: contralateral normal appearing region; t/c: ratio of tumor/contralateral.

J Magn Reson Imaging. Author manuscript; available in PMC 2017 November 01.

Table 2

Statistical results of quantitative DSC and iVASO measures from all 12 patients.

		DSC MRI		iVASO MRI	
		CBV (ml/100 ml)	MTT (s)	CBVa (ml/100 ml)	ATT (ms)
WHO grade II (n=6)					
Tumoral region		3.28±0.96 [f]	5.08±0.70	0.25±0.31	103.66±93.73
Contralateral region		2.62±0.77	4.92±0.48	0.97±0.51	417.28±106.56
Tumor/contralateral [a]		1.30±0.40	1.03±0.14	0.25±0.30	0.32±0.36
Relative change (%) [b]		25.27	3.05	−74.70	−75.20
Effect size [c]		0.76	0.25	−1.71	−3.13
Adjusted P [d]		0.15	0.60	0.03	0.01
SNR [e]	**tumor**	10.99±4.74		11.42±5.29	
	contralateral	11.29±2.74		11.17±6.61	
CNR [e]		2.82±0.91	0.34±0.12	−8.44±4.32	−8.49±4.37
WHO grade III (n=3)					
Tumoral region		4.37±1.82	5.54±1.01	0.72±0.91	327.59±392.57
Contralateral region		5.01±1.85	5.67±1.00	1.30±0.05	340.56±105.83
Tumor/contralateral		0.86±0.08	0.98±0.01	0.55±0.67	1.17±1.61
Relative change (%)		−12.80 *	−2.28	−44.62 *	−3.81
Effect size		−0.35	−0.13	−0.9	−0.05
Adjusted P		0.12	0.05	0.37	0.97
SNR	**tumor**	12.86±5.82		14.95±2.72	
	contralateral	11.19±5.68		10.31±3.88	
CNR [e]		−1.54±0.81	−0.27±0.13	−5.63±1.41	−0.48±0.15
WHO grade IV (n=3)					
Tumoral region		4.82±1.29	4.55±0.75	1.03±0.31	173.34±71.28
Contralateral region		2.49±1.39	4.86±0.32	0.59±0.29	550.58±218.98
Tumor/contralateral		2.36±1.27	0.93±0.11	1.88±0.42	0.36±0.18
Relative change (%)		93.73	−6.42	75.10	−68.50
Effect size		1.74	−0.54	1.49	−2.32
Adjusted P		0.21	0.41	0.001	0.12
SNR	**tumor**	10.58±4.99		10.31±2.84	
	contralateral	10.21±4.09		14.19±5.86	
CNR [e]		9.74±4.16	−0.67±0.31	9.20±3.21	−8.39±2.81

[a]The ratio was defined as (mean value in tumoral region / mean value in similar-sized contralateral region).

[b]Relative change was defined as 100 * (mean value in tumoral region – mean value in contralateral region) / (mean value in contralateral region) %.

[c] Effect size was estimated with Cohen's d = (mean value in tumoral region – mean value in contralateral region) / s, where s is the pooled standard deviation of the two groups.

[d] P-values from the paired two-sided t-Test between tumoral and contralateral regions. Adjusted for multiple comparisons with the Benjamini-Hochberg false discovery rate (FDR) procedure.

[e] Signal-to-noise ratio (SNR) was calculated on the original DSC images and iVASO difference images in each ROI (not on the CBV/MTT/CBVa/ATT maps). Contrast-to-noise ratio (CNR) was defined as SNR * relative change.

[f] mean±standard deviation

[*] Note that the negative average values of these parameters in the WHO grade III group were caused by the mix of oligodendroglioma (one patient) and anaplastic astrocytoma (two patients) cases. Please see Table 1 and text in Results and Discussion for more information.